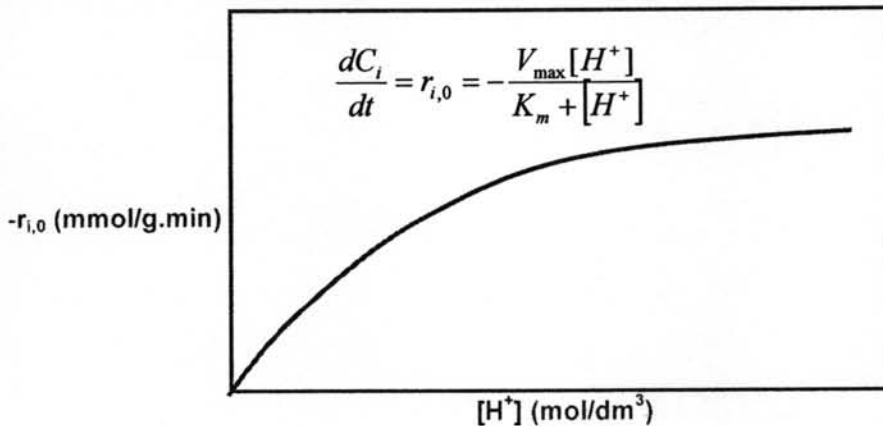


## CHAPTER IV

### RESULTS AND DISCUSSION

#### 4.1 Initial Dissolution Rate of Analcime in Different Acids

Analcime dissolution was carried out in different acids and the method of initial rates was used to find the kinetic parameters of the dissolution reaction. Samples were withdrawn from the reaction mixture at very short reaction times and analyzed for Si and Al concentration using AAS. The slope of concentration-time trajectory gave the initial dissolution rate of the species at the particular  $H^+$  molarity. The initial rates were found similarly for various  $H^+$  molarities ranging from 0.25M to 6M. Hartman and Fogler (2005, 2006) have shown that analcime dissolution in HCl follows the Langmuir-Hinshelwood rate law analogous to the Michaelis-Menten equation for enzymes (Figure 4.1). Linearizing the Michaelis-Menten equation gives the Hanes-Woolf plot (Fig 4.2). Working backwards, a good fit of the data to the Hanes-Woolf plot would imply that the Michaelis-Menten rate law is being followed. The experimental data for different acids were fit to the Hanes-Woolf plot. An excellent match was observed in all the three cases indicating that irrespective of the type of acid used, the dissolution follows the Michaelis-Menten rate law.



**Figure 4.1** Langmuir-Hinshelwood kinetics analogous to Michaelis-Menten equation

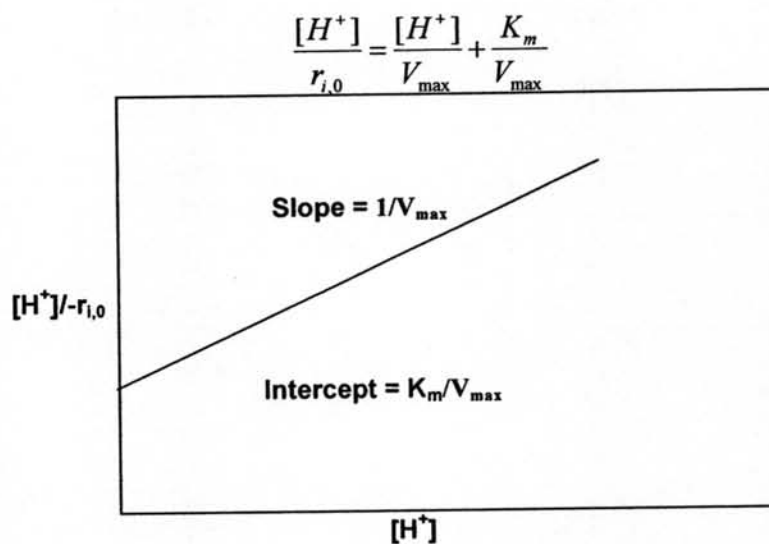


**Figure 4.2** Hanes-Woolf Plot (linearized Michaelis-Menten equation)

Figures 4.3-4.5 show the Hanes-Woolf plots for analcime dissolution in HCl, HBr and HNO<sub>3</sub> respectively.

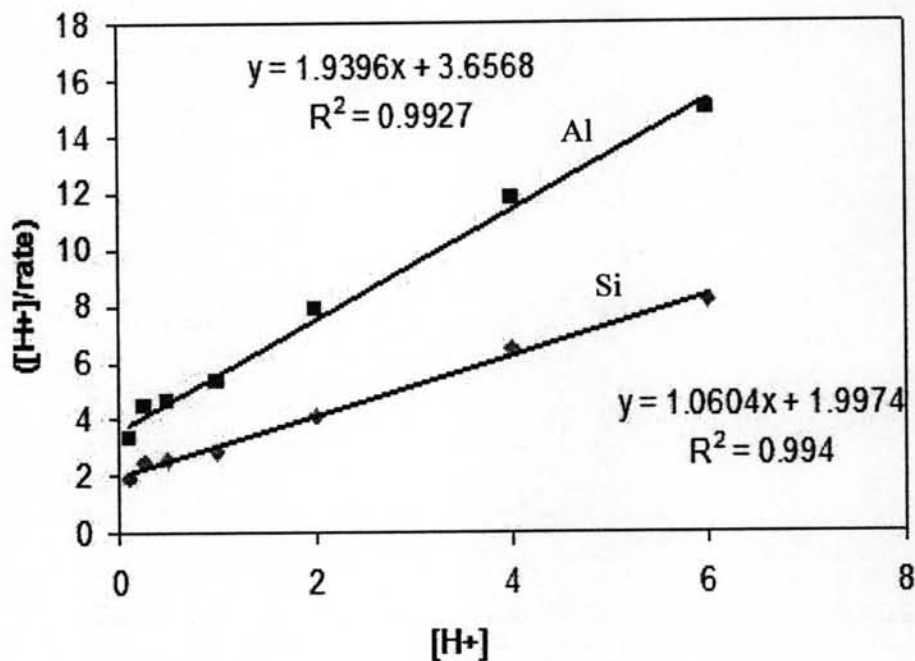


**Figure 4.3** Hanes-Woolf plot for analcime dissolution in HCl.

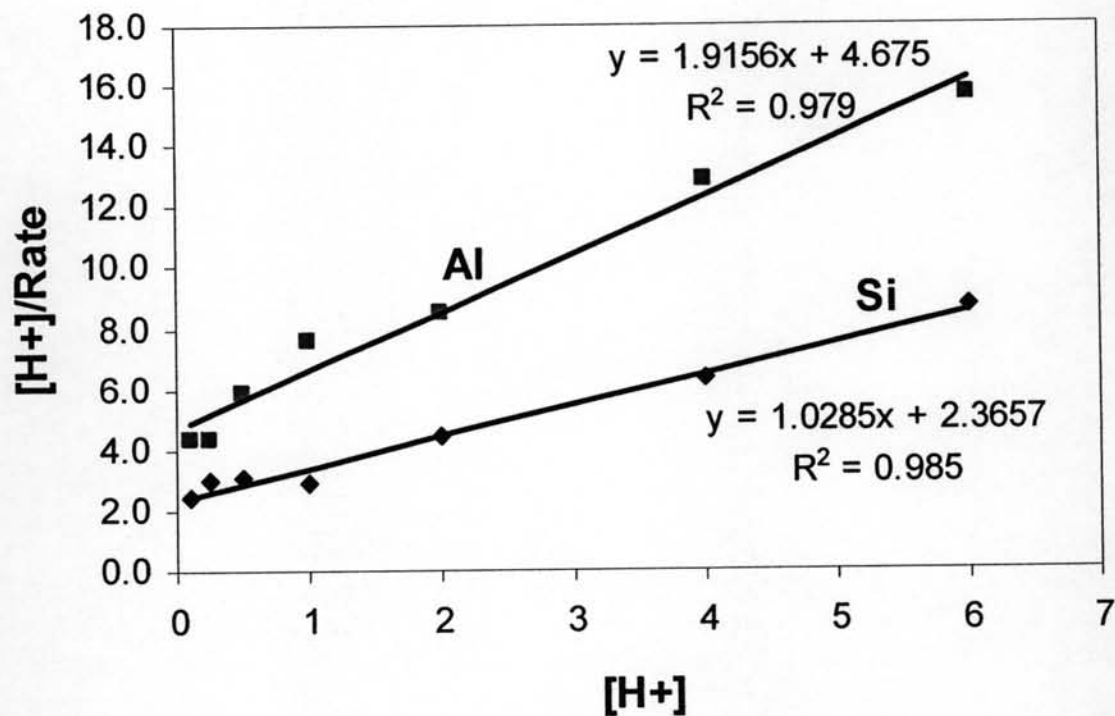


Figure 4.4 Hanes-Woolf plot for analcime dissolution in HBr

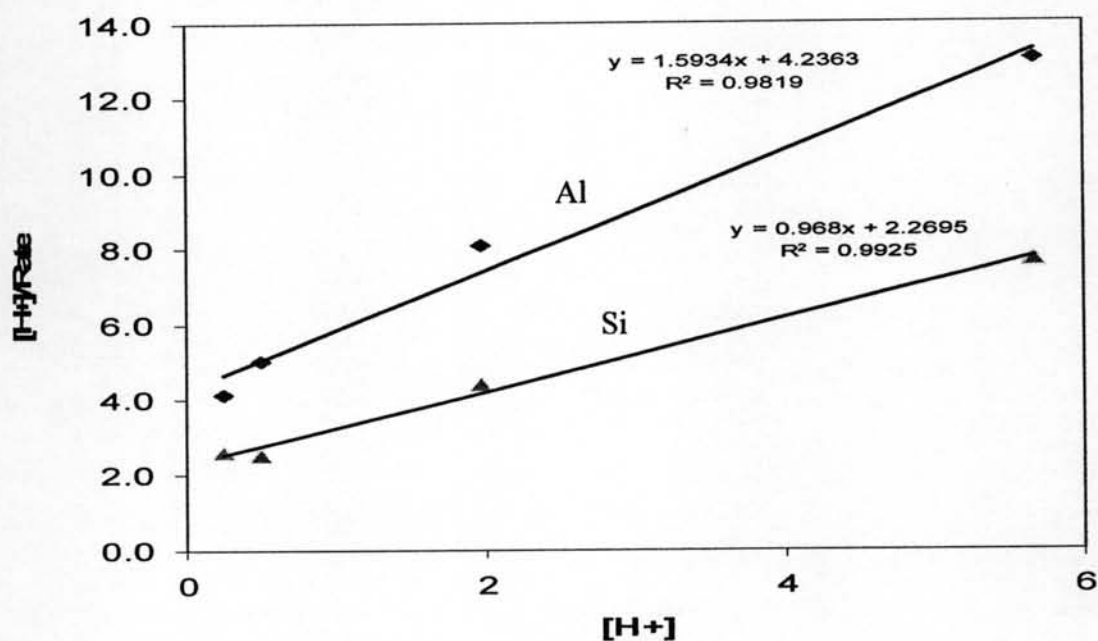


Figure 4.5 Hanes-Woolf plot for analcime dissolution in  $HNO_3$

Hartman and Fogler (2005) have suggested that the earlier empirical models for zeolite dissolution suggested by Rangsdottir (1993), Murphy *et al.* (1996) and Gdanski (2000) do not provide a good fit for analcime dissolution in HCl. As seen in the case of the acids studied Langmuir-Hinshelwood rate law seems to fit well.

The kinetic parameters for the three acids are shown in Table 4.1. The rates have been plotted against  $H^+$  concentration using the parameters from the Hanes-Woolf plot (Figures 4.3-4.5).

**Table 4.1** Kinetic parameters for Si and Al removal during analcime dissolution in different acids

Parameter	Acids					
	HCl		HBr		HNO <sub>3</sub>	
	Si	Al	Si	Al	Si	Al
$V_{max}$	0.943	0.516	0.972	0.522	1.033	0.627
$K_m$	1.883	1.885	2.3	2.44	2.345	2.659

The parameters found from the Hanes-Woolf plot were used to model the dissolution in different acids, shown by the solid lines in Figure 4.6 below. The plots for the other acids are shown in appendix A.

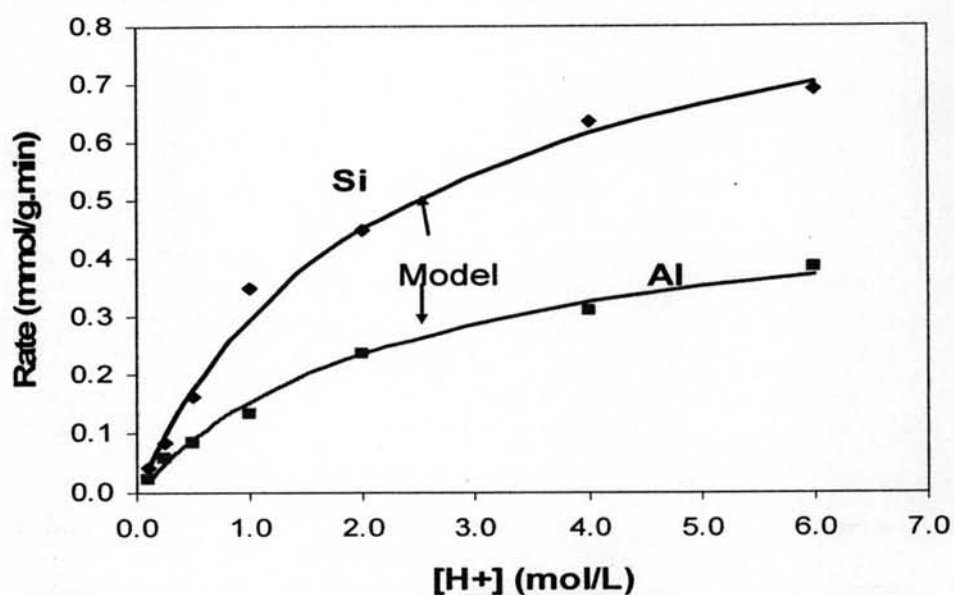


**Figure 4.6** Rate vs acid concentration for analcime dissolution in HBr

It is observed that the kinetic parameters do not vary much with the type of acid (Table 4.1). Thus it can be concluded that the dissolution rate does not depend on the anions of the acid, but is governed solely by the  $[H^+]$  concentration as shown in figures 4.7 and 4.8. This would imply that for a particular amount of analcime, the dissolution time required for the acids studied would be the same at the same acid concentration.

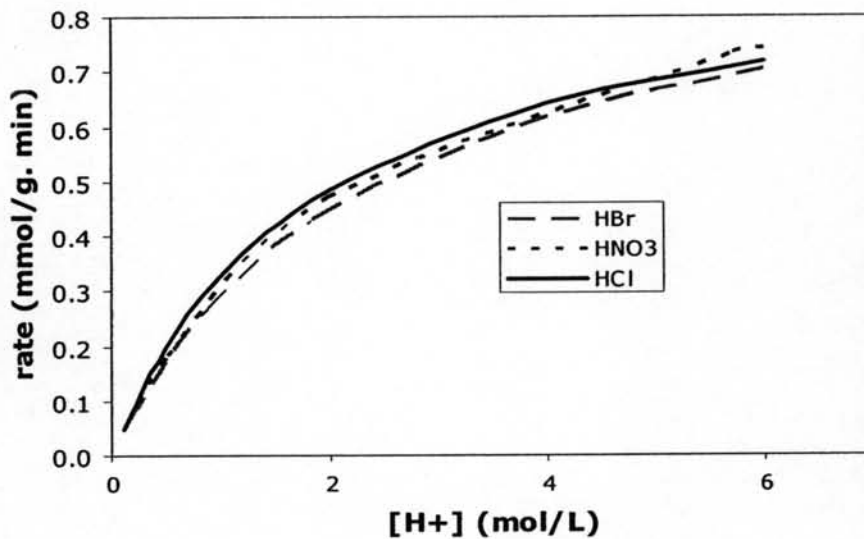


Figure 4.7 Rate comparison of Silicon removal for different acid concentrations.

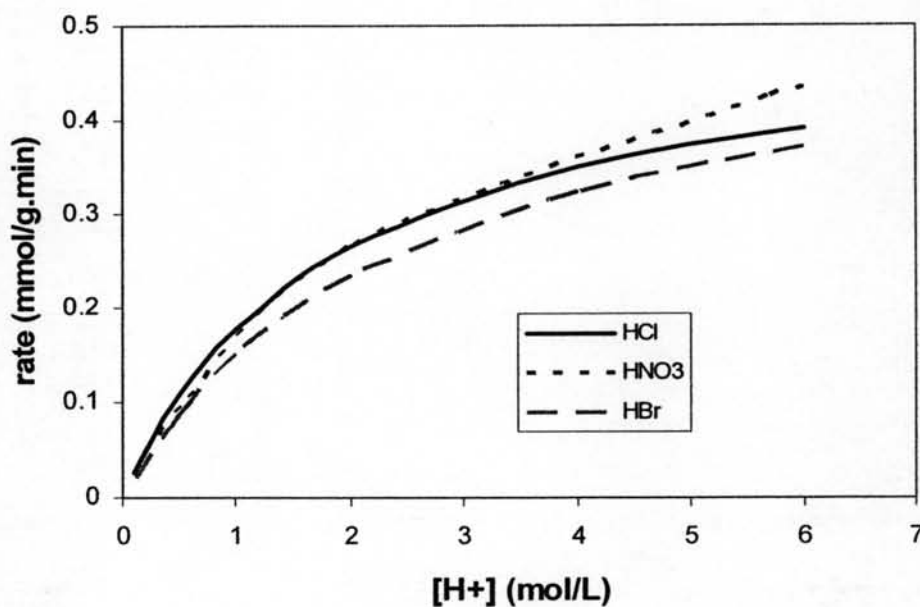
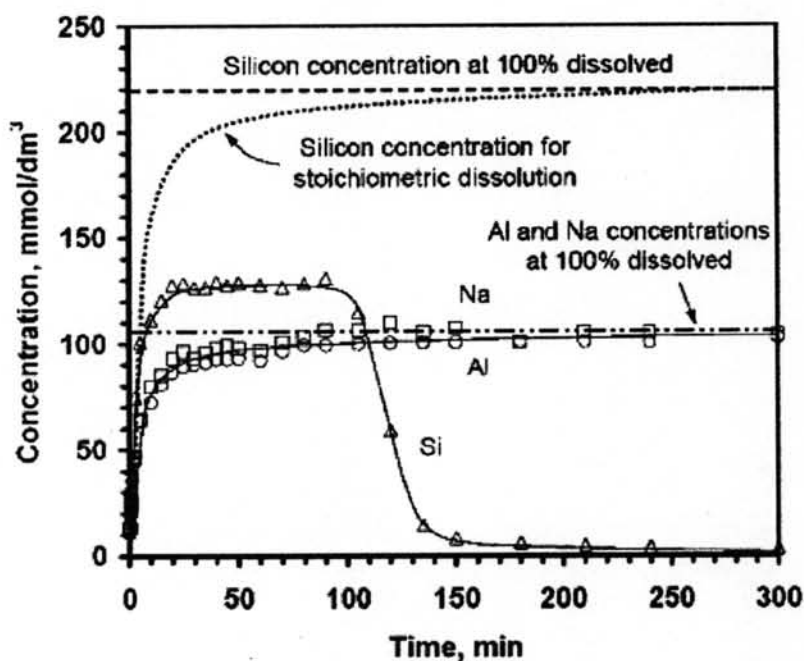


Figure 4.8 Rate comparison of Aluminum removal for different acids

## 4.2 Precipitation Experiments: Anion Effects

### 4.2.1 Precipitation experiments under base case conditions

In the base case experiments, 8 g of analcime was dissolved in 300 mL solution of 8M H<sup>+</sup> concentration at 5 °C and 500 rpm. From previous experiments done with HCl under these conditions, it was observed that Si concentration in solution increased as the dissolution proceeded after which reached a plateau (Hartman and Fogler, 2006). This plateau did not correspond to the complete dissolution of Si. After a certain lag time, the Si concentration drops down indicating the onset of Si precipitation from the solution (Figure 4.9)



**Fig 4.9** Base case experiment: Analcime dissolution in 8M HCl at 500 rpm and 5°C

Such a plateau before silica precipitation has also been reported by other researchers (Rothbaum and Rhode, 1979) in a homogeneous system. I was proposed that during the plateau, a slow formation of silica dimers takes place which then grow rapidly to give the precipitate. The cause of the plateau has not yet been established experimentally in our case. Preliminary results on light scattering show that there might actually be particle growth that might be taking place during the plateau. However, this hypothesis still needs to be substantiated by further experiments.

The experiments with different acids also show such a behavior as shown in Figure 4.10. However, the precipitation lag time and the plateau height differ with the type of acid being used. Among the acids with halogen anions, HCl shows the highest plateau and the longest lag time, while HI shows the least precipitation lag time and the lowest silica plateau. The plateau height in  $\text{HNO}_3$  is even slightly higher than the HCl, while the lag time is almost the same.

The halogen acids do show a certain trend in the lag time and the plateau height. They actually follow a decreasing trend for both, the lag time and the plateau height, with decreasing electronegativity. Another way to look into the behavior would be through the water binding strength of the anions. Sulfuric acid has a very high water binding strength, due to which it can reduce the solubility of silica more than any other acid and hence, possibly leading to a smaller precipitation lag time and a smaller silica plateau. However, there are anomalies in this theory as well. For example, nitric acid should have shown a smaller lag time and plateau, which it does not. So, this theory cannot explain the behavior completely and needs to be modified. However, for a first guess, it would be good to look into the binding strengths under the experimental conditions, which are not commonly encountered.

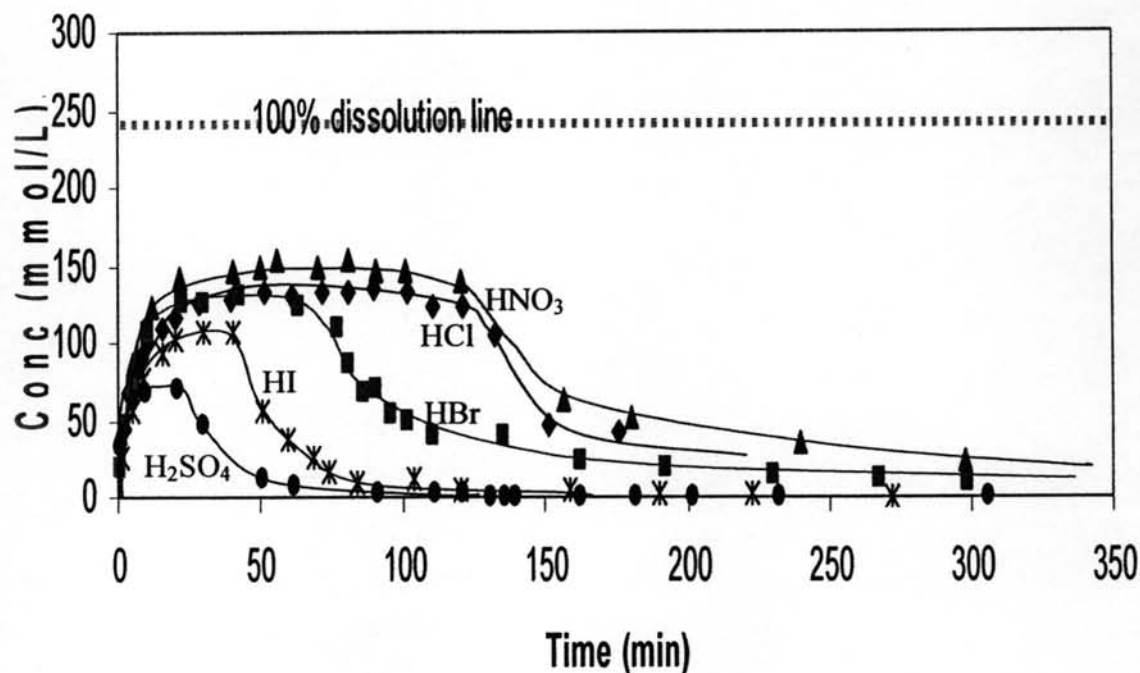


**Fig 4.10** Silica trajectories during analcime dissolution and silica precipitation in different acids

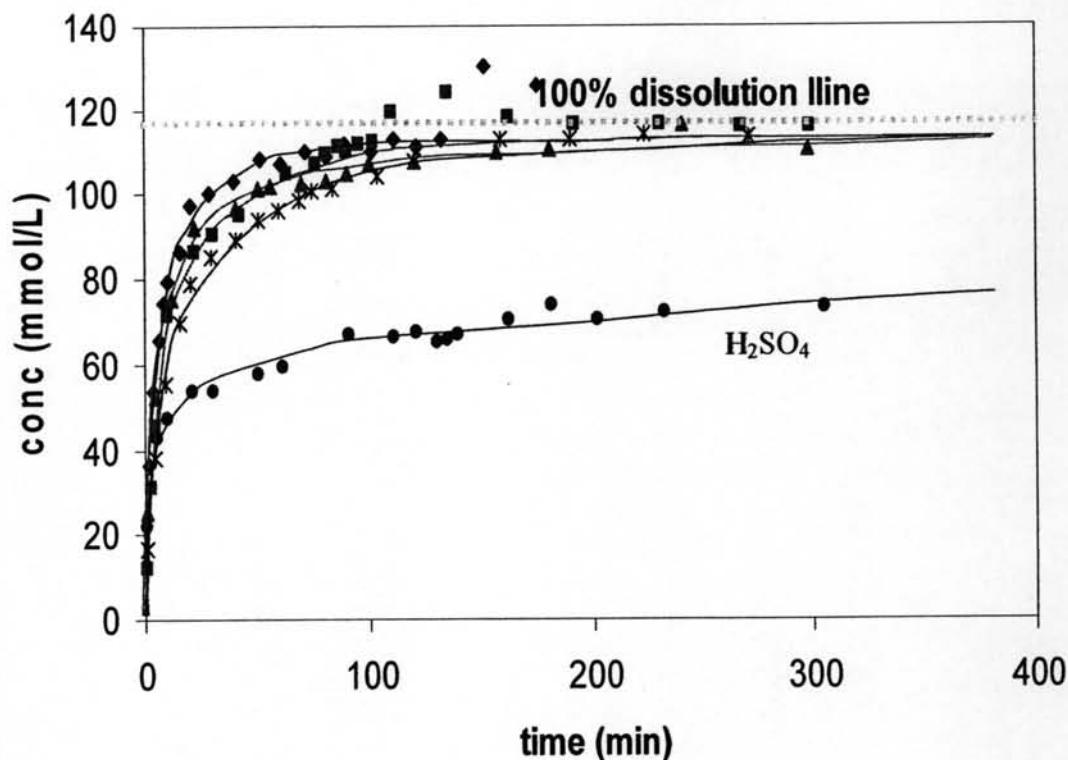


Fig 4.11 Aluminum trajectories during analcime dissolution and silica precipitation in different acids

#### 4.2.2 Experiments with Filtration of the Undissolved Particles

The particles were filtered out of the solution and examined under SEM in order to find compositional and structural differences while analcime was being dissolved in different acids. EDAX was used to analyze the surface composition of the particles. The SEM micrograph of the unreacted analcime particle is shown below (Figure 4.12). The EDAX gave a Si/Al ratio of 1.9 which is consistent with the AAS results.

Particles were filtered from the three zones of the experiment, namely, dissolution, silica plateau and precipitation and then washed before sputtering in order to remove any traces of acid (Fig 4.13). However, the SEM images of the unwashed particles didn't show a big difference, except for the sulfuric acid (appendix B).



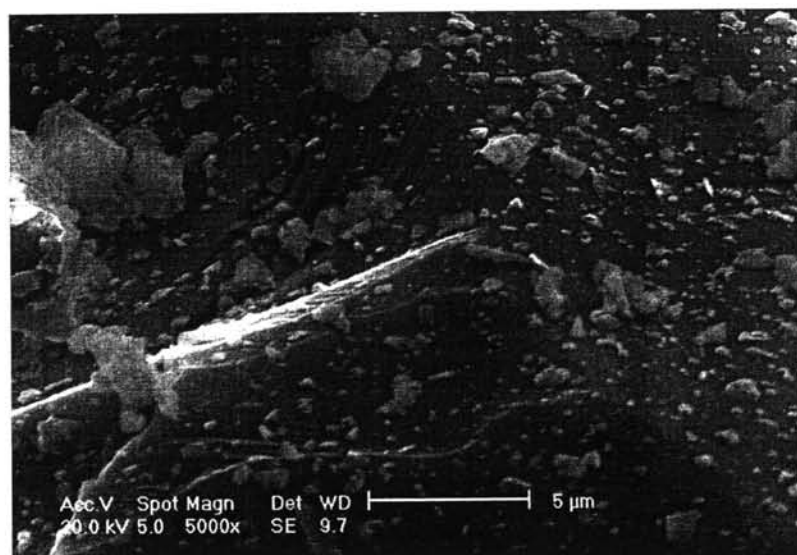


Fig 4.12 SEM micrograph of unreacted analcime

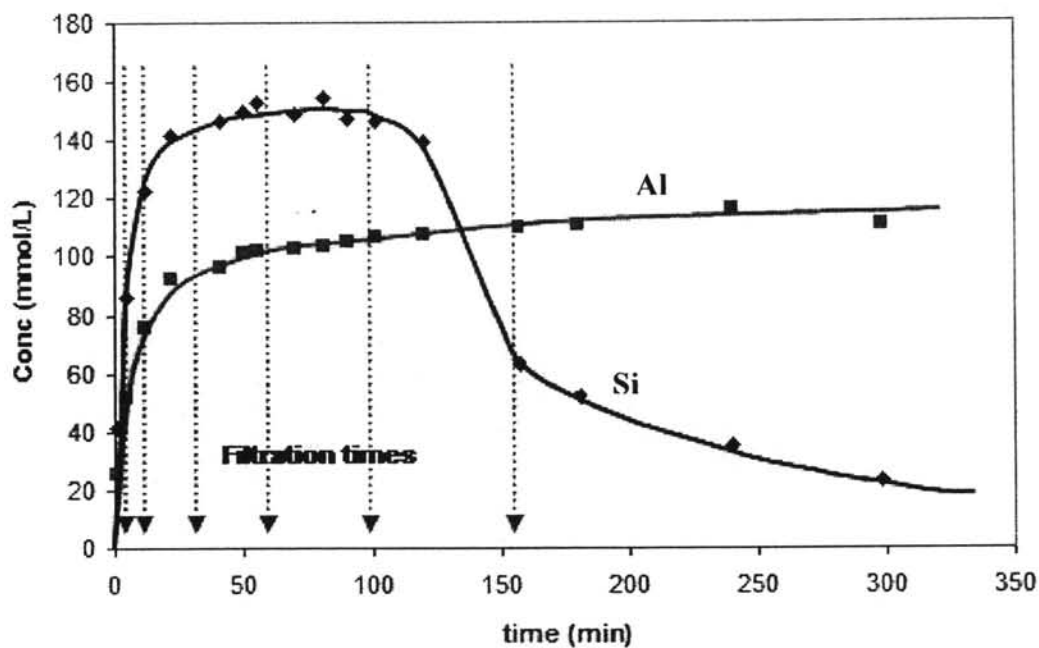
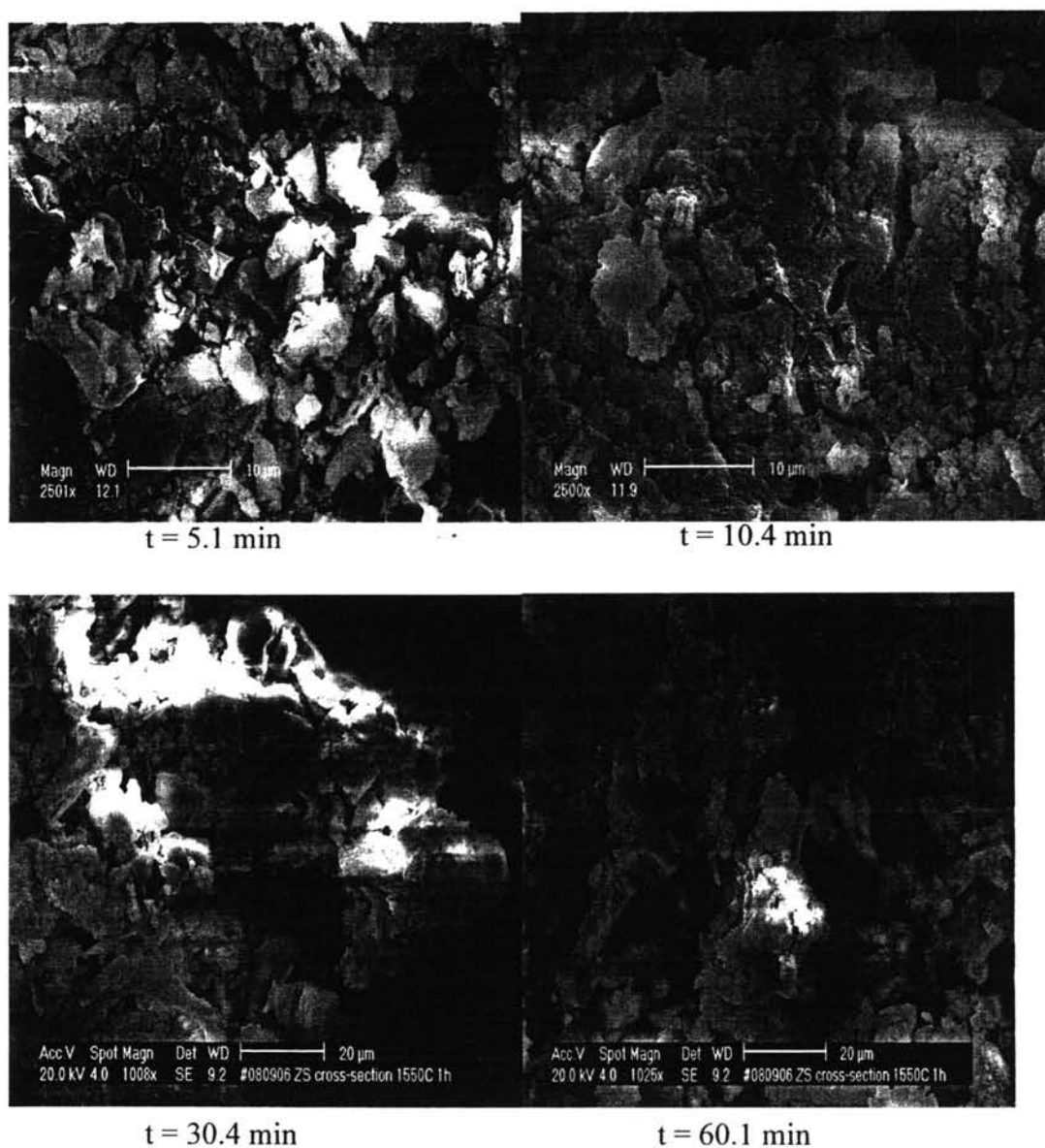
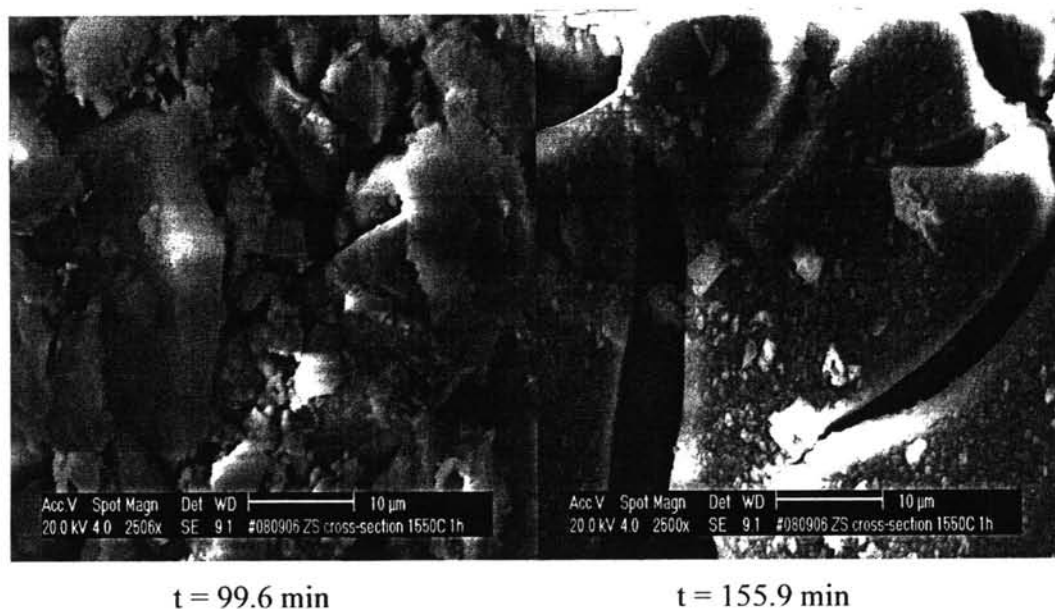


Fig 4.13 Filtration of undissolved particles from nitric acid solution (the dashed lines show the times at which filtration was carried out).

#### 4.2.2.1 SEM Micrographs Of The Filtered Particles In Nitric Acid

The SEM micrographs of the filtered particles at different times show the same trend for hydrochloric, nitric, hydrobromic and hydroiodic acids. First, etched channels and pits are formed in the particles. With time, these channels grow in size as the dissolution progresses (Figure 4.14). Then, after some time, the particles are completely broken and the undissolved particles remain in the solution. These particles remain undissolved till the entire time of experimentation and exist together with the subsequent silica precipitate.





**Fig 4.14** SEM micrographs of the undissolved particles in nitric acid

The SEM micrographs of the unwashed particles partially dissolved in sulfuric acid show a different behavior than those in the other acids. The particles look gellier and more interlinked than the other particles (Figure 4.15). It is probable that condensation of silanol bonds is taking place even during the dissolution phase and the plateau. However, more investigations through NMR or FT-IR studies are required to confirm such a behavior.

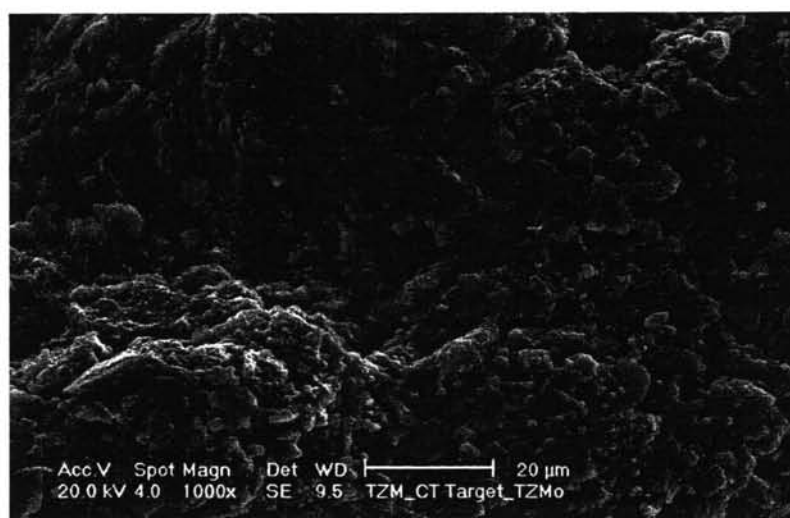


**Fig 4.15** SEM micrograph of undissolved particles in sulfuric acid

### 4.3 Aluminum Facilitated Dissolution of Analcime

The Si/Al ratio of the partially dissolved particles was analyzed using SEM-EDAX. Initially the ratio increases steeply and finally levels off at a final value of 15. Such a behavior was observed for analcime dissolution in HCl (Hartman, 2006). It was suggested that the dissolution of Si took place due to the removal of Al from the zeolite framework and once Al was completely removed, Si concentration did not increase any further. Also, there were traces of Al left in the partially dissolved particles which remained in the framework even after longer reaction times and did not get removed. This was suggested to be the reason behind the Si/Al ratio reaching a plateau. In Figure 4.16 below, such a behavior is observed for the partially dissolved particles in nitric acid as well, confirming the thesis that perhaps some Al is left in the framework.

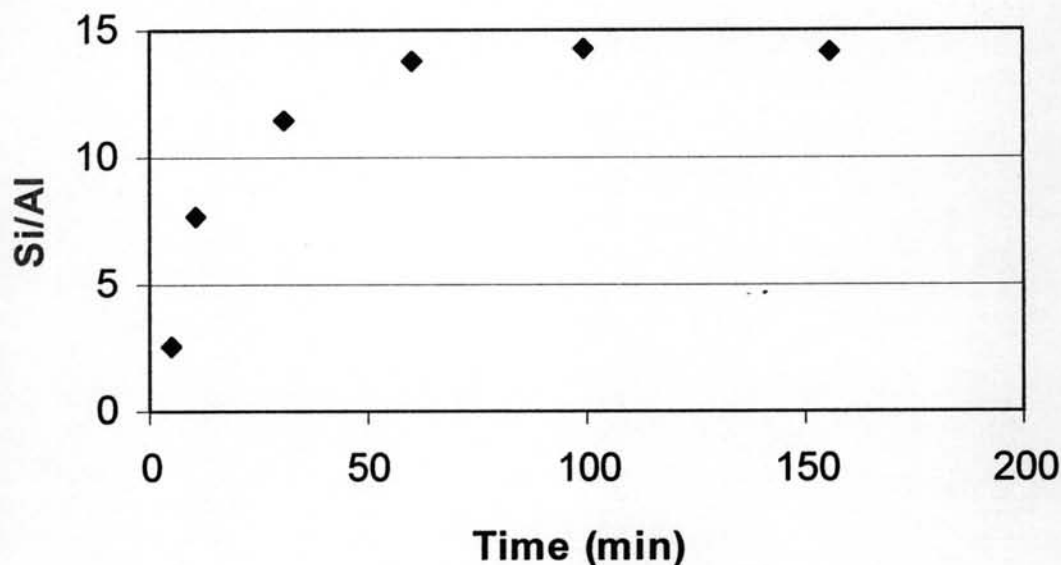


Fig 4.16 Si/Al ratio of the partially dissolved particles in nitric acid